Chapter 6

A Various Equation of State for Anisotropic Model of Compact Star

In this chapter, we obtain models of compact stars having pressure anisotropy on Finch Skea spacetime by considering generalized equation of state, whose particular cases are linear, quadratic, polytropic, Chaplygin and colour - flavor locked (CFL) equation of states. The physical viability of models is tested for strange star candidate 4U 1820 - 30 having mass $M = 1.58M_{\odot}$ and radius R = 9.1 km. All the models are found to be physically plausible. The stability of our model with various equation of state have been compared with work of Nasheeha *et. al.* [137].

6.1 Introduction

A compact star, as defined by general relativity, is a celestial object with an ultra-high density and a strong gravitational field. These stellar bodies, such as neutron stars and black holes, challenge our understanding of the cosmos and provide insights

into the extreme nature of spacetime. General relativity is crucial in modelling and understanding the physics regulating compact stars, unraveling the secrets of their structure, behaviour, and gravitational interactions. There are several models available in the literature describing relativistic compact objects.

At extremely high densities, the stellar interior may experience asymmetrical radial and tangential stresses and the pressure inside the stellar object may be anisotropic in nature studied by Ruderman [168]. Since the pioneering work of Bowers and Liang [28], various reasons for the appearance of anisotropy are available in the literature. Many authors have reported the origin and effects of local anisotropy on astrophysical objects (Herrera and Santos [75], Mak and Harko [120], Mak and Harko [119], Chan *et. al.* [33]). Anisotropy may occur due to type-3A superfluid (Harko and Mak [69]), phase transitions (Sokolov [182], Herrera and Nunez [72]), pion condensation (Sokolov [182], Herrera and Santos [74]), slow rotation of a fluid by Herrera and Santos [74], viscosity by Ivanov [82], strong electromagnetic fields (Weber [214], Martínez *et. al.* [130], Usov [209]).

Within the framework of general relativity, the equation of state relates the energy density, pressure, and other thermodynamic parameters to the curvature of spacetime. This interaction between the equation of state and general relativity is critical for adequately modelling compact objects such as neutron stars and black holes. By adopting a quadratic equation of state relating radial pressure to energy density, Maharaj and Takisa [127] provide innovative exact solutions to the Einstein-Maxwell set of equations. Malaver [131] used a quadratic equation of state to describe the interior of stellar configuration. Takisa *et. al.* [185] modeled a charged anisotropic relativistic star with a quadratic equation of state. Malaver and Kasmaei [132] proposed new relativistic star configuration with charged anisotropic fluid distribution. Ivanov [80] investigated relativistic static fluid spheres with a linear equation of

state. Maharaj and Thirukkanesh [126] examined the linear equation of state for matter distributions with anisotropic pressures in the presence of an electromagnetic field using the metric potential $g_{rr} = \frac{1}{a+bx^n}$. Maharaj *et. al.* [128] derived the solutions by considering charged anisotropic matter with a linear equation of state $p_r = \frac{1}{3}(\rho - \beta)$ consistent with quark stars. By selecting a particular form for one of the gravitational potentials and the electric field intensity, Ngubelanga *et. al.* [140] derived a new exact solution in isotropic coordinates. Ivanov [83] did an analytical study of anisotropic compact star models that are similar to charged isotropic solutions. Prasad and Jitendra [152] used a linear equation of state to study three different classes of innovative exact solutions for anisotropy factor by considering metric potential $e^{\lambda} = \frac{k(1+cr^2)}{k+cr^2}$ with $k < 0$ and $c > 0$. Recently Patel *et. al.* [155] investigated a new charged anisotropic solution on paraboloidal spacetime using a linear equation of state that is compatible with several compact stars.

Polytropic equations of state are useful in a wide range of astrophysical applications. Binnington and Poisson [23] used polytropic equation of state to define electric-type and magnetic-type love numbers in the context of a spherical body affected by an external tidal field. Chavanis [38] developed a simple universe model with a generalized equation of state $p = (\alpha + k\rho^{(1/n)})\rho c^2$ that has a linear component $p = \alpha\rho c^2$ and a polytropic component $p = k\rho^{(1+1/n)}c^2$. Takisa and Maharaj [184] studied charged anisotropic polytropic models. Herrera *et. al.* [77] investigated conformally flat spherically symmetric fluid distributions that meet a polytropic equation of state. Considering the polytropic equation of state Ngubelanga and Maharaj [139] investigated the Einstein-Maxwell system of equations in isotropic coordinates for anisotropic matter distributions in the presence of an electric field. Herrera *et. al.* [78] investigated the impact of modest fluctuations in local anisotropy of pressure and energy density on the incidence of cracking in spherical compact objects satisfying a polytropic equation of state. Azam *et. al.* [5] studied the theory of

Newtonian and relativistic polytropes with generalized polytropic equations of state with anisotropic fluid distribution in the presence of charge. Azam and Mardan [6] investigated the possibility of cracking in charged anisotropic polytropes with a generalized polytropic equation of state under two alternative assumptions. Recently, Nazar *et. al.* [136] proposed relativistic polytropic models of charged anisotropic compact objects.

Rahaman *et. al.* [165] examined singularity-free solutions for anisotropic charged fluids with the Chaplygin equation of state. Bhar *et. al.* [19] investigated closed-form solutions for modelling compact stars with interior matter distributions that obey a generalized Chaplygin equation of state. Prasad *et. al.* [151] proposed a new model of an anisotropic compact star in Buchdahl spacetime assuming the Chaplygin equation of state. Malaver and Iyer [133] investigated the analytical model of a compact star using a modified Chaplygin equation of state.

Nasheeha *et. al.* [137] have taken metric potential $g_{rr} = \frac{1+ar^2}{1+(a-b)r^2}$ for various equation of state viz. quadratic, linear, polytropic, Chaplygin, and color-flavor-locked equation of state. It is observed that the metric potential g_{tt} and many physical entities are not well-behaved in the case of $a = b$ for various equation of states viz. quadratic, linear, polytropic, Chaplygin, and color-flavor-locked equation of state. The reason is specified in Chapter 1. Hence we need to consider $a = b$ in $g_{rr} = \frac{1+ar^2}{1+(a-b)r^2}$ separately. We consider metric potential $g_{rr} = 1 + ar^2$ which is particular case of $g_{rr} = \frac{1+ar^2}{1+(a-b)r^2}$ considered by Nasheeha *et. al.* [137] when $a = b$. We develop new models for anisotropic stars using a generalized version of the nonlinear barotropic equation of state with a specific gravitational potential g_{rr} and demonstrate how it can be reduced to other types of equation of state to explain acceptable anisotropic matter distributions. Graphical analysis is done to investigate the physical acceptability of models.

6.2 The Field Equations

The static spherically symmetric spacetime metric in the interior of stellar configuration is given by

$$ds^2 = e^{\nu(r)}dt^2 - e^{\lambda(r)}dr^2 - r^2(d\theta^2 + sin^2\theta d\phi^2). \tag{6.1}$$

We take the energy-momentum tensor of the form

$$T_{ij} = (\rho + p_\perp)u_i u_j + p_\perp g_{ij} + (p_r - p_\perp)\chi_i\chi_j, \tag{6.2}$$

where ρ is the matter density, p_r is the radial pressure, $p_\perp$ is the tangential pressure, u^i is the four-velocity of the fluid and χ^i is a unit spacelike four-vector along the radial direction so that $u^i u_i = -1, \chi^i\chi_j = 1$ and $u^i\chi_j = 0$, with spacetime metric (6.1) and energy-momentum tensor (6.2), the Einstein's field equations takes the form

$$8\pi\rho = \frac{1 - e^{-\lambda}}{r^2} + \frac{e^{-\lambda}\lambda'}{r}, \tag{6.3}$$

$$8\pi p_r = \frac{e^{-\lambda}\nu'}{r} + \frac{e^{-\lambda} - 1}{r^2}, \tag{6.4}$$

$$8\pi p_\perp = e^{-\lambda}\left(\frac{\nu''}{2} + \frac{\nu'^2}{4} - \frac{\nu'\lambda'}{4} + \frac{\nu' - \lambda'}{2r}\right), \tag{6.5}$$

$$8\pi\sqrt{3}S = 8\pi p_r - 8\pi p_\perp. \tag{6.6}$$

where primes denote differentiation with respect to r. The system of equation (6.3-6.6) governs the behaviour of the gravitational field for an anisotropic fluid distribution.

6.3 Equation of State for Various Models

A generalized equation of state considered by Nasheeha *et. al.* [137] of the form

$$p_r = \tau\rho^{(1+\frac{1}{p})} + \eta\rho - \omega, \tag{6.7}$$

where τ, η, ω and p are real constants. If we put p=1 in equation (6.7), then it becomes a quadratic equation of state. If we put $\tau = 0$ in equation (6.7), then it becomes a linear equation of state. If we fix $\eta = 0$, in equation (6.7), then it becomes a polytrope with polytropic index p. If we set $p = \frac{-1}{2}$, $\omega = 0$ and $\tau = -\alpha$, in equation (6.7), then it becomes a Chaplygin equation of state. If we set $p = -2$, then it becomes color-flavor-locked (CFL)equation of state.

We solve Einstein's field equations (6.3 - 6.6) together with the equation of state (6.7), to obtain an anisotropic model with the equation of state. For solving the system (6.3-6.6), we have three equations with five unknowns (ρ, p_r, $p_\perp$, e^λ, e^ν). We are free to select any two of them to complete this system. As a result, there are ten different ways to select any two unknowns. There are four ways to choose the method, (i) choose ρ along with p_r (ii) select e^ν with Δ (iii) select e^λ and p_r and (iv) choose e^λ and equation of state, which is a relationship between matter density and radial pressure p_r.

To develop a physically reasonable model of the stellar configuration, we assume that the metric potential g_{rr} coefficient is expressed as e^λ given by

$$e^\lambda = 1 + ar^2, \tag{6.8}$$

by selecting this metric potential, the function e^λ is guaranteed to be finite, continuous, and well-defined within the range of stellar interiors.

$$\rho = \frac{a(3+ar^2)}{(1+ar^2)^2}, \tag{6.9}$$

$$p_r = \tau\left(\left(\frac{a(3+ar^2)}{(1+ar^2)^2}\right)^{(1+\frac{1}{p})} - \left(\frac{a(3+aR^2)}{(1+aR^2)^2}\right)^{(1+\frac{1}{p})}\right)+\eta\left(\frac{a(3+ar^2)}{(1+ar^2)^2} - \frac{a(3+aR^2)}{(1+aR^2)^2}\right), \tag{6.10}$$

$$p_\perp = \frac{a}{4\left(ar^2+1\right)^3}\left(f_1+f_2+\frac{ar^2(f_3+f_4)^2}{\left(aR^2+1\right)^4}+\frac{2(f_3+f_5+f_6)}{\left(aR^2+1\right)^2}\right), \tag{6.11}$$

$$x = \left(\frac{a\left(ar^2+3\right)}{\left(ar^2+1\right)^2}\right)^{1/p},$$

$$y = \left(\frac{a\left(aR^2+3\right)}{\left(aR^2+1\right)^2}\right)^{1/p},$$

$$f_1 = -\frac{4ar^2\tau x\left(ar^2+5\right)}{p}+\frac{2a\left(r^2(-5\eta+\tau(x-6y)+1)+R^2(5\eta+6\tau x-\tau y+2)\right)2+6\tau(x-y)}{\left(aR^2+1\right)^2}-4(1+ar^2),$$

$$f_2 = \frac{2a^2\left(-3r^4(\eta+\tau y)+2r^2R^2(\tau(x-y)+1)+R^4(3\eta+3\tau x+1)\right)-2a^3r^2R^2\left(r^2(\eta+\tau y)-R^2(\eta+\tau x+1)\right)}{\left(aR^2+1\right)^2},$$

$$f_3 = a\left(r^2(-5\eta+\tau x-6\tau y+1)+R^2(5\eta+6\tau x-\tau y+2)\right)+3\tau(x-y)+1,$$

$$f_4 = a^2\left(-3r^4(\eta+\tau y)+2r^2R^2(\tau x-\tau y+1)+R^4(3\eta+3\tau x+1)\right)-a^3r^2R^2\left(r^2(\eta+\tau y)-R^2(\eta+\tau x+1)\right),$$

$$f_5 = a^4r^4R^2\left(R^2(\eta+\tau x+1)-3r^2(\eta+\tau y)\right)+a^3\left(-9r^6(\eta+\tau y)+r^4R^2(-5\eta+2\tau x-7\tau y+2)+2r^2R^4\right),$$

$$f_6 = a^2\left(r^4(-20\eta+\tau x-21\tau y+1)-r^2R^2(5\eta+5\tau y-4)+R^4(3\eta+3\tau x+1)\right).$$

$$e^\nu = C\ (1+ar^2)^\eta exp(f_7+f_8), \tag{6.12}$$

$$f_7 = \frac{p\tau x\left(ar^2+1\right)Hypergeometric\ {}_2F_1\left(\frac{1}{p}-1,-\frac{1}{p};\frac{1}{p};-\frac{2}{ar^2+1}\right)}{2(p-1)\left(\frac{2}{ar^2+1}+1\right)^{1/p}}-\frac{\left(ar^2+1\right)^2\left(aR^2+3\right)(\eta+\tau y)}{4\left(aR^2+1\right)^2},$$

$$f_8 = \frac{(\eta+1)\,(ar^2+1)}{4} - \frac{\mathrm{p}\tau Hypergeometric\ {}_2F_1\left(-\frac{1}{p},\frac{1}{p};1+\frac{1}{p};-\frac{2}{ar^2+1}\right)}{\left(\frac{2}{ar^2+1}+1\right)^{1/p}}.$$

where, C is a constant of integration.

$$C = \frac{1}{(1+aR^2)^{(\eta+1)}} exp\left(\frac{\left(aR^2+3\right)(\eta+\tau y) - 2(\eta+1)\left(aR^2+1\right)}{4} + \frac{2(p-1)p\tau y f_9}{2(p-1)\left(\frac{2}{aR^2+1}+1\right)^{1/p}}\right), \tag{6.13}$$

$$f_9 = Hypergeometric\ {}_2F_1\left(-\frac{1}{p},\frac{1}{p};1+\frac{1}{p};-\frac{2}{aR^2+1}\right)$$
$$-\left(aR^2+1\right) Hypergeometric\ {}_2F_1\left(\frac{1}{p}-1,-\frac{1}{p};\frac{1}{p};-\frac{2}{aR^2+1}\right).$$

The mass function within the sphere of radius R for the metric potential equation (6.8) is given by

$$M = \frac{aR^3}{2(1+aR^2)}. \tag{6.14}$$

In our generated model, equation (6.12) is the solution for different values of p. Subsequently, we consider the different cases in the following sections which are of physical interest.

6.3.1 Quadratic Equation of State

If we set p = 1 then equation (6.7) takes the form of quadratic equation of state

$$p_r = \tau\rho^2 + \eta\rho - \omega, \tag{6.15}$$

$$e^{\lambda} = 1 + ar^2, \tag{6.16}$$

$$\rho = \frac{a(3+ar^2)}{(1+ar^2)^2}, \tag{6.17}$$

$$p_r = \tau\left(\left(\frac{a(3+ar^2)}{(1+ar^2)^2}\right)^2 - \left(\frac{a(3+aR^2)}{(1+aR^2)^2}\right)^2\right) + \eta\left(\frac{a(3+ar^2)}{(1+ar^2)^2} - \frac{a(3+aR^2)}{(1+aR^2)^2}\right), \tag{6.18}$$

$$p_\perp = \frac{a}{4\left(ar^2+1\right)}\left(f_{10}+f_{11}+f_{12}+f_{13}\right), \tag{6.19}$$

$$f_{10} = \frac{16a\tau - 2ar^2(a\tau+2\eta)}{\left(ar^2+1\right)^2} - \frac{2ar^2+4+2a\eta r^2-(4a\tau+8\eta)}{ar^2+1} + 4(\eta+1),$$

$$f_{11} = (2ar^2 - 4\left(ar^2+1\right) - 8a^2\tau r^2)p_{14} + \frac{16a\tau - 8a^2\tau r^2}{\left(ar^2+1\right)^3},$$

$$f_{12} = 4ar^2\left(-f_{14} - \frac{a\tau+2\eta}{\left(ar^2+1\right)^2} - \frac{8a\tau}{\left(ar^2+1\right)^3} - \frac{12a\tau}{\left(ar^2+1\right)^4}\right),$$

$$f_{13} = ar^2\left((-ar^2+1)f_{14} + \frac{a\tau+2\eta}{ar^2+1} + \frac{4a\tau}{\left(ar^2+1\right)^2} + \frac{4a\tau}{\left(ar^2+1\right)^3} + \eta + 1\right)^2,$$

$$f_{14} = \frac{\left(aR^2+3\right)\left(a^2R^2\left(\tau+\eta R^2\right)+a\left(3\tau+2\eta R^2\right)+\eta\right)}{\left(aR^2+1\right)^4},$$

$$e^\nu = C\left(1+ar^2\right)^{\left(\frac{a\tau+2\eta}{2}\right)} exp(f_{15}), \tag{6.20}$$

$$f_{15} = -\frac{a\tau}{(1+ar^2)^2} - \frac{2a\tau}{(1+ar^2)} + \frac{(1+ar^2)(1+\eta)}{2}$$
$$-\frac{(3+aR^2)(1+ar^2)^2\left(\eta+a^2R^2(\tau+R^2\eta)+a(3\tau+2R^2\eta)\right)}{4(1+aR)^4},$$

where,

$$C = \frac{exp\left(-\frac{a\tau}{(1+aR^2)^2} - \frac{2a\tau}{(1+aR^2)} + \frac{(1+aR^2)(1+\eta)}{2} - \frac{(3+aR^2)\left(\eta+a^2R^2(\tau+R^2\eta)+a(3\tau+2R^2\eta)\right)}{4(1+aR)^2}\right)}{\left(1+aR^2\right)^{\left(\frac{a\tau+2\eta}{2}+1\right)}}. \tag{6.21}$$

The same metric potential is used by Sharma and Ratanpal [179], but assuming radial pressure in the form of $8\pi p_r = \frac{p_0(1-\frac{r^2}{R^2})}{R^2(1+\frac{r^2}{R^2})^2}$. Similarly Feroze and Siddiqui [56] used same ansatz for metric potential g_{rr} considering charged anisotropic matter with quadratic equation of state.

6.3.2 Linear Equation of State

If we set $\tau = 0$, equation (6.7) becomes

$$p_r = \eta\rho - \omega, \tag{6.22}$$

$$e^{\lambda} = 1 + ar^2, \tag{6.23}$$

$$\rho = \frac{a(3+ar^2)}{(1+ar^2)^2}, \tag{6.24}$$

$$p_r = \eta\left(\frac{a(3+ar^2)}{(1+ar^2)^2} - \frac{a(3+aR^2)}{(1+aR^2)^2}\right), \tag{6.25}$$

$$p_{\perp} = \frac{a\left(4(1+\eta) + \frac{8\eta-4-2ar^2(1+\eta)}{1+ar^2} + 2\eta\left(-\frac{ar^2\left(aR^2+3\right)}{\left(aR^2+1\right)^2} - \frac{2\left(ar^2+1\right)\left(aR^2+3\right)}{\left(aR^2+1\right)^2} - \frac{6ar^2}{\left(ar^2+1\right)^2}\right)\right)}{4(1+ar^2)}$$

$$+\frac{ar^2\left(\frac{2\eta}{ar^2+1} - \frac{\eta\left(ar^2+1\right)\left(aR^2+3\right)}{\left(aR^2+1\right)^2} + \eta + 1\right)^2}{4(1+ar^2)}, \tag{6.26}$$

$$e^{\nu} = C\,(1+ar^2)^{\eta} exp\left(\frac{(1+ar^2)(1+\eta)}{2} - \frac{\eta(3+aR^2)(1+ar^2)^2}{(1+aR^2)^2}\right), \tag{6.27}$$

where,

$$C = \frac{exp\left(\frac{-2+\eta-aR^2(2+\eta)}{4}\right)}{(1+aR^2)^{(\eta+1)}}. \tag{6.28}$$

which is similar to the solution of Thomas and Pandya [200] with $a = \frac{1}{L^2}$.

6.3.3 Polytropic Equation of State

When p = 2 and $\eta = 0$, equation (6.7) takes a polytropic form

$$p_r = \tau\rho^{(3/2)} - \omega, \tag{6.29}$$

so Einstein's field equations become,

$$p_r = \tau\left(\left(\frac{a(3+ar^2)}{(1+ar^2)^2}\right)^{(3/2)} - \left(\frac{a(3+aR^2)}{(1+aR^2)^2}\right)^{(3/2)}\right), \tag{6.30}$$

$$p_\perp = \frac{a\left(-2\left(ar^2+1\right)^3\left(aR^2+1\right)^2 f_{16} - ar^2\left(ar^2+1\right)^2 f_{17}\left(2\left(aR^2+1\right)^2 - f_{17}\right) + \frac{2\left(aR^2+1\right)^2}{l} f_{18}\right)}{4\left(ar^2+1\right)^5\left(aR^2+1\right)^4}, \tag{6.31}$$

$$l = \sqrt{\frac{a\left(ar^2+3\right)}{\left(ar^2+1\right)^2}}, \quad m = \sqrt{\frac{a\left(aR^2+3\right)}{\left(aR^2+1\right)^2}},$$

$$f_{16} = a^3\left(mr^4R^2\tau - r^2R^4(l\tau+1)\right) + a^2\left(-2r^2R^2(l\tau - m\tau + 1) + R^4(1-3l\tau) + 3mr^4\tau\right)$$

$$-3l\tau + 3m\tau + 1 - a\left(r^2(l\tau - 6m\tau + 1) + R^2(6l\tau - m\tau - 2)\right),$$

$$f_{17} = a^3\left(r^2R^4(l\tau+1) - mr^4R^2\tau\right) + a^2\left(2r^2R^2(l\tau - m\tau + 1) + R^4(3l\tau+1) - 3mr^4\tau\right)$$

$$+a\left(r^2(l\tau - 6m\tau + 1) + R^2(6l\tau - m\tau + 2)\right) + 3\tau(l-m) + 1,$$

$$f_{18} = a^5\left(-9lmr^{10}\tau + lr^8R^2(2-13m\tau) + 4lr^6R^4 - 5r^4R^4\tau\right) + l(1-3m\tau)$$

$$+a^4\left(lr^8(1-39m\tau) + 2lr^6R^2(4-11m\tau) + 2r^4\left(3lR^4 - 5R^2\tau\right) - 12r^2R^4\tau\right)$$

$$+a^2\left(6lr^4(1-9m\tau) + r^2\left(lR^2(8-7m\tau) - 12\tau\right) + lR^4 + 18R^2\tau\right)$$

$$+al\left(r^2(4-21m\tau) + R^2(2-m\tau+9\tau)\right) + a^6lr^8R^2\left(R^2 - 3mr^2\tau\right)$$

$$+a^3\left(2lr^6(2-33m\tau) + r^4\left(-6lR^2(3m\tau-2) - 5\tau\right) + 4r^2\left(lR^4 - 6R^2\tau\right) + 9R^4\tau\right),$$

$$e^\nu = C\ exp\left(\frac{f_{19}}{4\left(aR^2+1\right)^2}\right), \tag{6.32}$$

$$f_{19} = 2 - 3m\tau + a^3r^2R^2(-r^2m\tau + R^2(2+4l\tau)) + a(r^2(2+4l\tau-6m\tau) + R^2(4-m\tau))$$

$$+a^2(2R^4-3r^4m\tau+2r^2R^2(2+4l\tau-m\tau)-6\sqrt{2}\sqrt{a}\tau\left(aR^2+1\right)^2\tanh^{-1}\left(\frac{(ar^2+1)\,m}{\sqrt{2}\sqrt{a}}\right),$$

where,

$$C=\frac{\exp\left(-\frac{a^3R^6(3\tau m+2)+a^2R^4(3\tau m+6)+a^2R^2(6-3\tau m)-3\tau m-6\sqrt{2}\sqrt{a}\tau\left(aR^2+1\right)^2\tanh^{-1}\left(\frac{\left(aR^2+1\right)m}{\sqrt{2}\sqrt{a}}\right)+2}{4\left(aR^2+1\right)^2}\right)}{aR^2+1}.$$

This is the new solution for this gravitational potential in polytropic equation of state.

6.3.4 Chaplygin Equation of State

If we set $p=-\frac{1}{2},\tau=-\alpha$ and $\omega=0$ then equation (6.7) becomes Chaplygin equation of state as

$$p_r=\eta\rho-\frac{\alpha}{\rho}, \tag{6.33}$$

$$p_\perp=\frac{f_{20}+f_{21}+f_{22}}{4a^2\left(ar^2+1\right)^3\left(ar^2+3\right)^2}, \tag{6.34}$$

$$f_{20}=a^8r^{10}\left(\eta-\alpha r^4+1\right)^2+2a^7r^8\left(6\eta^2+11\eta+4\alpha^2r^8-\alpha(10\eta+13)r^4+5\right)$$

$$+2a^2\alpha r^2\left(-9\eta+14\alpha r^4-48\right)+4a\alpha\left(2\alpha r^4-3\right)+\alpha^2r^2,$$

$$f_{21}=2a^6r^6\left(27\eta^2+43\eta+14\alpha^2r^8-3\alpha(13\eta+22)r^4+18\right)+2a^3\left(54\eta+28\alpha^2r^8-3\alpha(14\eta+47)r^4\right),$$

$$f_{22}=2a^5r^4\left(54\eta^2+75\eta+28\alpha^2r^8-4\alpha(19\eta+40)r^4+27\right)$$

$$+a^4r^2\left(9\left(9\eta^2+16\eta+3\right)+70\alpha^2r^8-2\alpha(79\eta+205)r^4\right),$$

$$e^{\nu} = C\ (1+ar^2)^{\eta}(3+ar^2)^{\frac{4\alpha}{a^2}} exp\left(\frac{-(1+ar^2)(10\alpha - ar^2\alpha + a^2(-3+r^4\alpha-3\eta))}{6a^2}\right), \tag{6.35}$$

where,

$$C = \frac{(3+aR^2)^{(\frac{-4\alpha}{a^2})} exp\left(-(\frac{-(1+aR^2)(10\alpha - aR^2\alpha + a^2(-3+R^4\alpha-3\eta))}{6a^2})\right)}{(1+aR^2)^{(\eta+1)}}. \tag{6.36}$$

6.3.5 CFL Equation of State

When the internal structure of a compact star formed of strange matter is in the CFL phase, CFL equation of state is used. If we set $p = -2$, then equation (6.7) becomes CFL equation of state (Thirukkanesh and Ragel [195], Rocha *et. al.* [167])

$$p_r = \tau\rho^{\frac{1}{2}} + \eta\rho - \omega, \tag{6.37}$$

$$p_{\perp} = -\frac{f_{23}+f_{24}+f_{25}+f_{26}}{36\,(ar^2+1)}, \tag{6.38}$$

$$f_{23} = \frac{108a^2\eta r^2}{(ar^2+1)^2} + \frac{18a\eta\,(aR^2+3)\,(ar^2\,(ar^2+1))}{(aR^2+1)^2} - 36a(\eta+1+r^2\tau p) - 48\tau\left(ar^2+2\right)p,$$

$$f_{24} = \frac{18a^2(\eta+1)r^2 + 24ar^2\tau\,(ar^2+2) + 36a(1-2\eta) - 6ar^2\tau p\,(ar^2+5)}{ar^2+1},$$

$$f_{25} = \frac{6a^2r^2\tau\,(ar^2+5)\,(4\,(ar^2+2)-(ar^2+5))}{(ar^2+1)^3\,p} + 18q\tau(3ar^2+2) + 12\tau\left(ar^2+5\right)p,$$

$$f_{26} = r^2\left(-3a(\eta+1) - \frac{6a\eta}{ar^2+1} + 3q(1+ar^2)(q\eta+\tau) - 4\tau\left(ar^2+2\right)p + \tau\left(ar^2+5\right)p\right)^2,$$

$$e^{\nu} = C\ (1+ar^2)^{\eta}$$

$$exp\left(\frac{\tau\left(a^2r^4+4ar^2+3\right)p}{3a}+\frac{2(\eta+1)\left(ar^2+1\right)}{4}-\frac{\eta\left(ar^2+1\right)^2\left(aR^2+3\right)}{4\left(aR^2+1\right)^2}-\frac{\tau\left(ar^2+1\right)^2q}{4a}\right), \tag{6.39}$$

where,

$$C=\frac{exp\left(-\frac{\tau q\left(a^2R^4+4aR^2+3\right)}{3a}-\frac{(\eta+1)\left(aR^2+1\right)}{2}+\frac{\eta\left(aR^2+3\right)}{4}+\frac{p\tau\left(aR^2+1\right)^2}{4a}\right)}{(aR^2+1)^{(\eta+1)}}. \tag{6.40}$$

All of the physical plausibility conditions are representing in the next section.

6.4 Matching conditions

At the boundary of the star $r = R$, we match the interior metric with the Schwarzschild exterior spacetime metric.

$$ds^2=\left(1-\frac{2M}{r}\right)dt^2-\left(1-\frac{2M}{r}\right)^{-1}dr^2-r^2(d\theta^2+sin^2\theta d\phi^2), \tag{6.41}$$

which leads to

$$\left(1-\frac{2M}{R}\right)^{-1}=1+aR^2=e^{\lambda} \tag{6.42}$$

$$\left(1-\frac{2M}{R}\right)=e^{\nu} \tag{6.43}$$

$$M=\frac{aR^3}{2(1+aR^2)} \tag{6.44}$$

where e^{ν} is given in (6.20), (6.27), (6.32), (6.35), (6.39) for quadratic, linear, polytropic, Chaplygin, and color-flavor-locked equation of state, respectively. We use a graphical approach to examine and physically validate the remaining physical conditions for a realistic star by fixing the radius R = 9.1 km and mass $M = 1.58M_{\odot}$ in analogy with the strange star candidate 4U 1820-30. Therefore, using a graphical

presentation, we demonstrate that the models created for parameters a = 0.01 for all types of equation of states satisfy the majority of the physical conditions given above. Table (6.1) lists the additional parameters selected for various equations of states.

Table 6.1: The numerical values of the τ, η, ω and constant(a) for the compact star 4U 1820-30.

Equation of states	τ	η	ω	**a**	$\rho(\mathbf{0})$ **(MeV fm^{-3})**	$\rho(\mathbf{R})$ **(MeV fm^{-3})**
Quadratic	0.1	0.15	1	0.01	903.407	344.942
Linear	0	0.15	1	0.01	903.407	344.942
Polytropic	1.5	0	0	0.01	903.407	344.942
Chaplygin	0.1	0.1	0	0.01	903.407	344.942
CFL	0.01	0.15	0	0.01	903.407	344.942

Table 6.2: The numerical values of the strong energy condition and redshift at the centre as well as surface, and adiabatic index at the surface for the compact star 4U 1820-30.

Equation of states	$\rho - \mathbf{p_r} - \mathbf{2p_\perp}$ **(r=0)**	$\rho - \mathbf{p_r} - \mathbf{2p_\perp}$ **(r=R)**	$\mathbf{Z_{(r=0)}}$ **(Redshift)**	$\mathbf{Z_{(r=R)}}$ **(Redshift)**	$\mathbf{\Gamma_{(r=0)}}$ **(Adiabatic Index)**
Quadratic	645.152	274.575	0.707848	0.352072	1.79312
Linear	652.098	273.485	0.706874	0.352072	1.76766
Polytropic	365.402	316.69	0.747744	0.352072	2.3529
Chaplygin	602.444	325.82	0.722774	0.352072	1.49029
CFL	592.312	295.712	0.718688	0.352072	1.73714

6.5 Conditions for Physical Acceptability

Following are the condition for model to be physically plausible.

(i) $\rho(r) \geq 0, \quad p_r(r) \geq 0, \quad p_\perp(r) \geq 0, \qquad$ for $0 \leq r \leq R$

(ii) $\frac{d\rho}{dr} \leq 0, \quad \frac{dp_r}{dr} \leq 0, \quad \frac{dp_\perp}{dr} \leq 0, \qquad$ for $0 \leq r \leq R$

(iii) $0 \leq \frac{dp_r}{d\rho} \leq 1\ , \quad 0 \leq \frac{dp_\perp}{d\rho} \leq 1, \quad$ for $0 \leq r \leq R$

Table 6.3: The numerical values of the $\frac{d\rho}{dr}, \frac{dp_r}{dr}$ and $\frac{dp_\perp}{dr}$ at centre as well as surface for the compact star 4U 1820-30.

Equation	$\frac{\mathbf{d\rho}}{\mathbf{dr}}$ **(r=0)**	$\frac{\mathbf{d\rho}}{\mathbf{dr}}$ **(r=R)**	$\frac{\mathbf{dp_r}}{\mathbf{dr}}$ **(r=0)**	$\frac{\mathbf{dp_r}}{\mathbf{dr}}$ **(r=R)**	$\frac{\mathbf{dp_\perp}}{\mathbf{dr}}$ **(r=0)**	$\frac{\mathbf{dp_\perp}}{\mathbf{dr}}$ **(r=R)**
Quadratic	0	-52.283	0	-7.96223	0	-6.3821
Linear	0	-52.283	0	-7.84246	0	-6.29418
Polytropic	0	-52.283	0	-12.5903	0	-8.71212
Chaplygin	0	-52.283	0	-13.5936	0	-23.8567
CFL	0	-52.283	0	-10.285	0	-10.6138

Table 6.4: The numerical values of the $\frac{dp_r}{d\rho}$ at centre as well as surface and $\frac{dp_\perp}{d\rho}$ at centre as well as surface for the compact star 4U 1820-30.

Equation of states	$\frac{\mathbf{dp_r}}{\mathbf{d\rho}}$ **(r=0)**	$\frac{\mathbf{dp_\perp}}{\mathbf{d\rho}}$ **(r=0)**	$\frac{\mathbf{dp_r}}{\mathbf{d\rho}}$ **(r=R)**	$\frac{\mathbf{dp_\perp}}{\mathbf{d\rho}}$ **(r=R)**	$(\nu_\mathbf{t}^\mathbf{2} - \nu_\mathbf{r}^\mathbf{2})$ **(r=0)**	$(\nu_\mathbf{t}^\mathbf{2} - \nu_\mathbf{r}^\mathbf{2})$ **(r=R)**
Quadratic	0.156	0.10074	0.152291	0.122068	-0.05526	-0.030223
Linear	0.15	0.0904949	0.15	0.120387	-0.0595051	-0.029613
Polytropic	0.389711	0.492584	0.24081	0.166634	0.102873	-0.074176
Chaplygin	0.148953	0.0757274	0.26	0.456299	-0.0732256	0.1962
CFL	0.178868	0.132934	0.204667	0.203006	-0.045934	-0.001661

(iv) $\quad \rho - p_r - 2p_\perp \geq 0, \qquad$ for $0 \leq r \leq R$

(v) $\quad \Gamma > \frac{4}{3}, \qquad$ for $0 \leq r \leq R$

Let's now examine the physical acceptability of the models created using five distinct types of equations of states.

In our models, for all types of equation of state $(e^\nu)'_{(r=0)} = (e^\lambda)'_{(r=0)} = 0, e^{\lambda(0)} = 1$ and e^ν becomes for

Quadratic equation of state :

$$e^{\nu(0)} = C\ exp\left[-\frac{\left(aR^2+3\right)\left(a^2R^2\left(\tau+\eta R^2\right)+a\left(3\tau+2\eta R^2\right)+\eta\right)}{4\left(aR^2+1\right)^4} - 3a\tau + \frac{\eta+1}{2}\right],$$

Linear equation of state :

$$e^{\nu(0)} = C\ exp\left[\frac{\omega+1}{2} - \frac{\omega\left(aR^2+3\right)}{4\left(aR^2+1\right)^2}\right],$$

Polytropic equation of state :

$$e^{\nu(0)} = C\ exp\left[\frac{2a^2R^4+aR^2\left(4-\tau\sqrt{\frac{a\left(aR^2+3\right)}{\left(aR^2+1\right)^2}}\right)-3\tau\sqrt{\frac{a\left(aR^2+3\right)}{\left(aR^2+1\right)^2}}+3i\sqrt{2}\tau\sqrt{a}\left(\pi+i\log\left(2\sqrt{6}+5\right)\right)\left(aR^2+1\right)^2+2}{4\left(aR^2+1\right)^2}\right],$$

Chaplygin equation of state :

$$e^{\nu(0)} = C\ exp\left[\frac{a^2(-(-3\eta-3))-10\alpha+24\alpha\log(3)}{6a^2}\right],$$

CFL equation of state :

$$e^{\nu(0)} = C\ exp\left[\frac{1}{4}\left(-\frac{\eta\left(aR^2+3\right)}{\left(aR^2+1\right)^2}-\frac{\tau\sqrt{\frac{a\left(aR^2+3\right)}{\left(aR^2+1\right)^2}}}{a}+\frac{4\sqrt{3}\tau}{\sqrt{a}}+2(\eta+1)\right)\right],$$

which are constants. The gravitational potentials are regular at the origin for all types of equations of state, satisfying requirements. In all kinds of equation of states, Fig.(6.1), Fig.(6.2), and Fig.(6.3) show that monotonically decreasing density, radial pressure, and tangential pressure from the centre to the surface of the star. Additionally, the density, radial pressure, and tangential pressure at the centre are positive. Fig.(6.2) shows that the radial pressure disappears at the star's boundary, at R = 9.1 km for all types of equation of state.

6.5.1 Energy Condition

The most crucial requirement for our model is to be a physically plausible, i.e. strong energy condition (SEC).

$$SEC : \rho - p_r - 2p_\perp \geq 0. \tag{6.45}$$

Table(6.2) shows the values of $\rho - p_r - 2p_\perp$ at a centre as well as the surface of the star.

6.5.2 Causality and Stability Conditions

(i) Causality Condition:

The causality condition demands that $0 \leq \frac{dp_r}{d\rho} \leq 1$ and $0 \leq \frac{dp_\perp}{d\rho} \leq 1$ at all interior

points of the star. Fig.(6.4) and Fig.(6.5) demonstrate that all equation of state models satisfy the causality criterion because the square of the radial and tangential sound speeds obeys the condition throughout the star's interior. For the compact star 4U 1820-30, the values of the $\frac{dp_r}{d\rho}, \frac{dp_\perp}{d\rho}$ at the centre and surface are provided in Table (6.4). For the stability of a star it is required to satisfy the condition $-1 \leq \frac{dp_\perp}{d\rho} - \frac{dp_r}{d\rho} \leq 1$. Abreu *et. al.* [1] have demonstrated that the ratio of variations in anisotropy to energy density for some specific dependent perturbations may be explained in terms of the difference in sound speeds. i.e. $\frac{\delta\Delta}{\delta\rho} \sim \frac{dp_\perp}{d\rho} - \frac{dp_r}{d\rho}$, and for physically reasonable models $|\frac{dp_\perp}{d\rho} - \frac{dp_r}{d\rho}| \leq 1$, implies that the magnitude of perturbations in anisotropy should always be smaller than those in density ($i.e. |\delta\Delta| \leq |\delta\rho|$). According to research by Abreu *et. al.* [1], a criterion based on the $\frac{dp_\perp}{d\rho} - \frac{dp_r}{d\rho}$ can be used to evaluate the relative magnitude of density and anisotropy perturbations and to assess the stability of bounded distributions that may cause instabilities that cause the configuration to crack, collapse, or expand. Fig.(6.10) shows that for the models with linear, quadratic, and CFL equations of states, the condition is satisfied everywhere in the interior of the stars. According to the theorem used by Ratanpal [161], if $8\pi\sqrt{3}S = p_r - p_\perp$ is a decreasing function of r, then the stellar configuration is potentially stable. It has been observed that the stellar models with linear and quadratic equation of state are potentially stable as the work of Nasheeha *et. al.* [137]. The models with Chaplygin equation of state are potentially unstable as in the work of Nasheeha *et. al.* [137]. However, stellar model with CFL equation of state are potentially stable in our case and potentially unstable in work of Nasheeha *et. al.* [137]. Further the stellar models with polytropic equation of state are potentially unstable in our case and potentially stable in work of Nasheeha *et. al.* [137].

(ii) Relativistic Adiabatic Index:

The adiabatic index which is defined as

$$\Gamma = \left(\frac{\rho + p_r}{p_r}\right)\frac{dp_r}{d\rho}, \tag{6.46}$$

is related to the stability of a relativistic anisotropic stellar configuration. If the adiabatic index, which physically describes the stiffness of the equation of state for a given density, is larger than 4/3, then any star configuration will continue to be stable. The first person to look at this was Chandrasekhar [35], who used equation (6.46) to show that, in the context of general relativity, the Newtonian lower limit $\frac{4}{3}$ has a large impact. Later, a number of researchers including Heintzmann and Hillebrandt [71], Hillebrandt and Steinmetz [79], Barreto *et. al.* [10], Chan *et. al.* [32], Doneva and Yazadjiev [51], Moustakidis [135] investigated the adiabatic index within a dynamically stable stellar system in the presence of an infinitesimal radial adiabatic perturbation. We have graphically depicted the nature of the relativistic adiabatic index variation for the quadratic, linear, polytropic, Chaplygin, and CFL equation of state in Fig.(6.8). Inside the stellar interior, the profile is monotonically increasing and greater than 4/3 everywhere. The value of the adiabatic Index is shown in Table (6.2).

6.5.3 Gravitational Redshift

The gravitational redshift z_G should be monotonically decreasing towards the boundary of the star. The central redshift z_G and boundary redshift z_G must be positive and finite. That is,

$$z_G = \sqrt{\frac{1}{e^{\nu}}} - 1. \tag{6.47}$$

For the compact star 4U 1820-30, the values of the gravitational redshift at the centre and surface are provided in Table (6.2).

6.5.4 Stability under Three Forces

Three forces, including gravitational force (F_g), hydrostatic force (F_h), and anisotropy force (F_a), can be used to confirm the static equilibrium of a star model. In the interior of the star, the sum of these forces must be zero.

$$F_g + F_h + F_a = 0, \tag{6.48}$$

which is formulated from the Tolman-Oppenheimer-Volkoff (TOV) equation

$$-\frac{M_G(r)(\rho + p_r)}{r^2} e^{(\lambda-\nu)/2} - \frac{dp_r}{dr} + \frac{2}{r}(p_\perp - p_r) = 0, \tag{6.49}$$

where the effective gravitational mass $M_G(r)$ is given by

$$M_G(r) = \frac{1}{2} r^2 e^{\frac{(\nu-\lambda)}{2}} \nu', \tag{6.50}$$

from the equation (6.48),(6.49) and (6.50), it can be written

$$F_g = -\frac{\nu'}{2}(\rho + p_r),$$

$$F_h = -\frac{dp_r}{dr},$$

$$F_a = \frac{2}{r}(p_\perp - p_r).$$

Fig.(6.11), Fig.(6.12), Fig.(6.13), Fig.(6.14), and Fig.(6.15) show, the hydrostatic balance behaviour of anisotropic fluid spheres for models created with quadratic, linear, and CFL equation of states respectively. It is obvious from the graphs that F_h, F_a, and F_g maintain the system's equilibrium in all cases. In this way, a positive anisotropy factor (Δ) brings a repulsive force into the arrangement that works to balance the gravitational gradient created by gravitational force F_g. The gravita-

tional collapse of the structure onto a point singularity is prevented by the existence of this anisotropic force repulsive in nature.

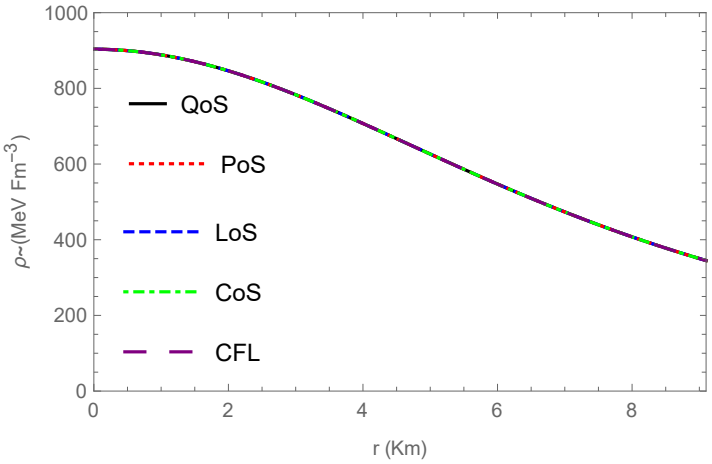

Figure 6.1: Variation of density against radial variable r.

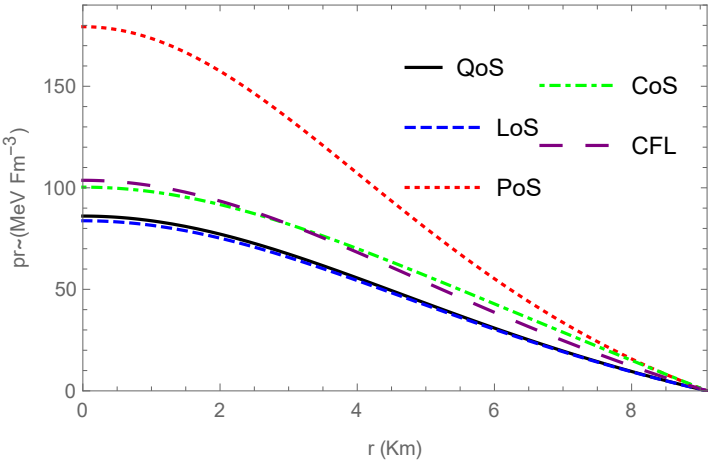

Figure 6.2: Variation of radial pressures against radial variable r.

6.6 Discussion

It is observed that the work of Nasheeha *et. al.* [137] does not give the exact solution for all equations of state linear, quadratic, polytrope, Chaplygin, and color-flavor-locked for metric potential $g_{rr} = \frac{1+ar^2}{1+(a-b)r^2}$ in the case of $a = b$. We develop new

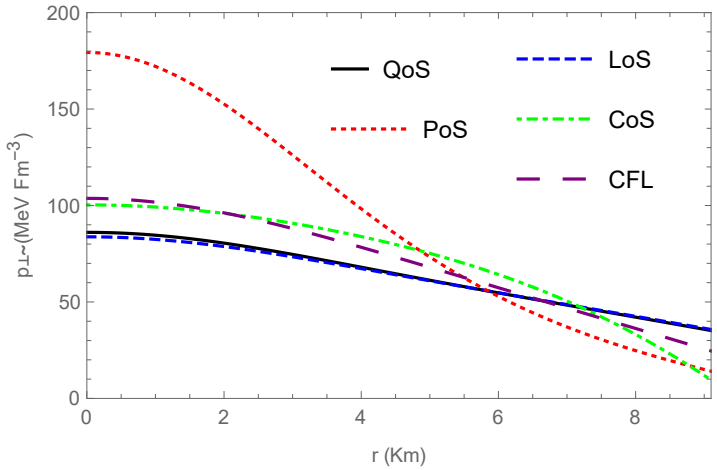

Figure 6.3: Variation of tangential pressures against radial variable r

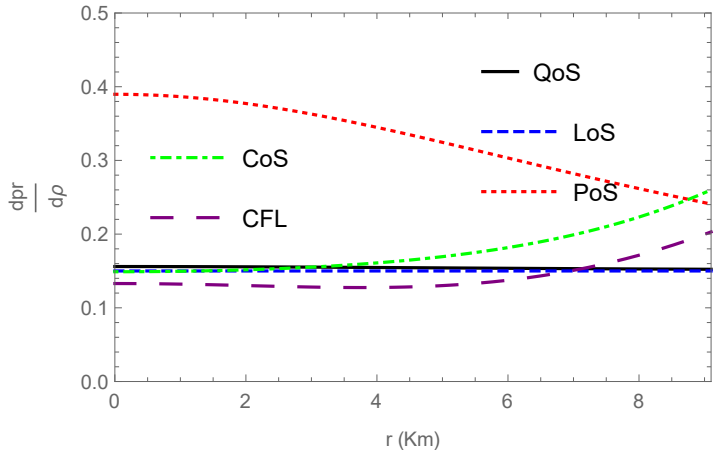

Figure 6.4: Variation of $\frac{dp_r}{d\rho}$ against radial variable r.

models for anisotropic stars using a generalized version of the nonlinear barotropic equation of state with a specific gravitational potential $g_{rr} = 1 + ar^2$. A generalized form of equation of state of the kind $p_r = \tau\rho^{(1+\frac{1}{p})} + \eta\rho - \omega$ helped us to solve the Einstein's field equations to describe static spherically symmetric anisotropic stars. By fixing the parameters involved in the equation of state, we then extracted models with different types of equations of state, including linear, quadratic, polytrope, Chaplygin, and color-flavor-locked. By fixing the radius R = 9.1 km and mass $M = 1.58M_{\odot}$ in analogy with the strange star candidate 4U 1820-30, the physical

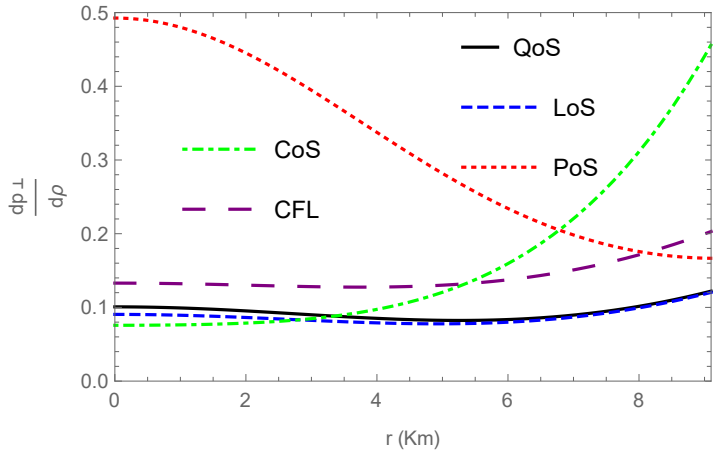

Figure 6.5: Variation of $\frac{dp_\perp}{d\rho}$ against radial variable r.

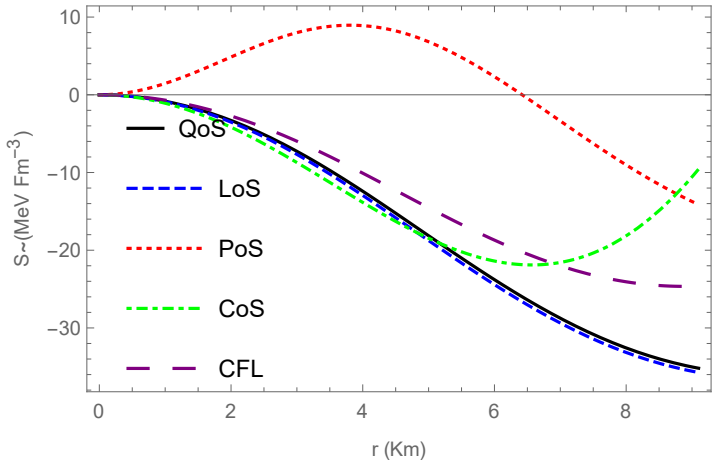

Figure 6.6: Variation of anisotropy against radial variable r.

accuracy of the generated models was evaluated.

In Fig. (6.1) we have shown the variation of density for the star 4U 1820-30. It is clear from the graph that the density is decreasing throughout the distribution. In Fig.(6.2) and Fig.(6.3), we have shown the variation of radial and tangential pressure throughout the star. It can be seen that both pressures are decreasing radially outward. For all varieties of the equation of state, the tangential pressure is not zero at the surface while the radial pressure vanishes at the surface. In Fig.(6.4) and Fig.(6.5), we have displayed the variation of $\frac{dp_r}{d\rho}$ and $\frac{dp_\perp}{d\rho}$ against r.

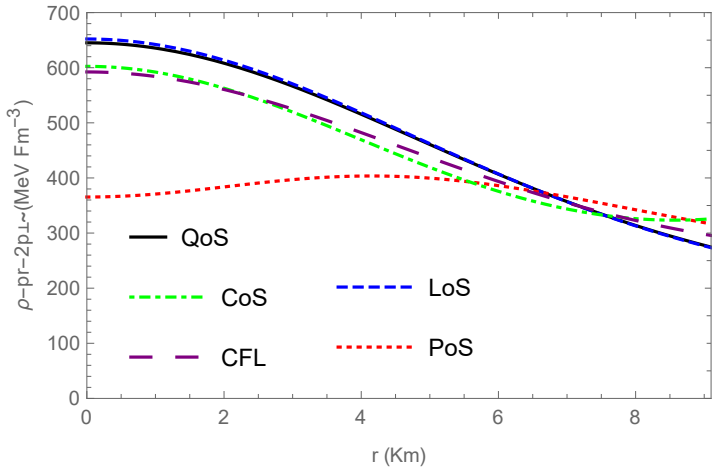

Figure 6.7: Variation of strong energy condition against radial variable r.

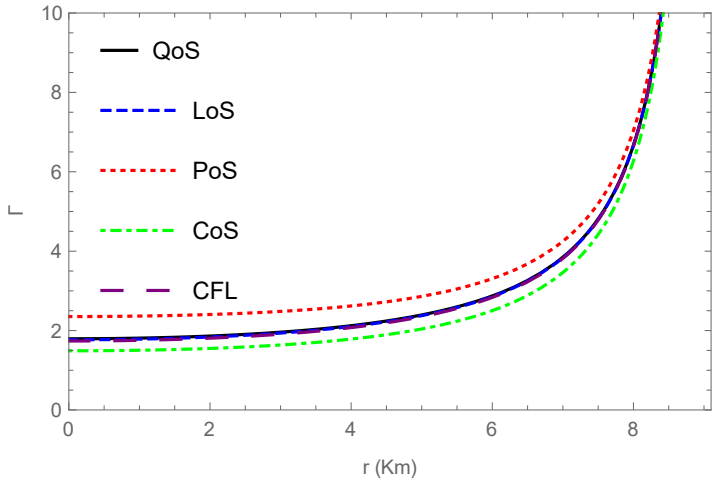

Figure 6.8: Variation of adiabatic Index against radial variable r.

Both quantities satisfy the restriction $0 < \frac{dp_r}{d\rho} < 1$ and $0 < \frac{dp_\perp}{d\rho} < 1$ indicating that the square of sound speed is less than the speed of light throughout the star.

The variation of anisotropy is shown in Fig.(6.6). According to the theorem used by Ratanpal [161], if $8\pi\sqrt{3}S = p_r - p_\perp$ is a decreasing function of r, then the stellar configuration is potentially stable. It has been observed that the stellar models with linear, quadratic and CFL equation of state are potentially stable in our case according to Fig.(6.6). It can be noticed that anisotropy vanishes at the centre and decreases towards the boundary for quadratic, linear, and CFL equation of states.

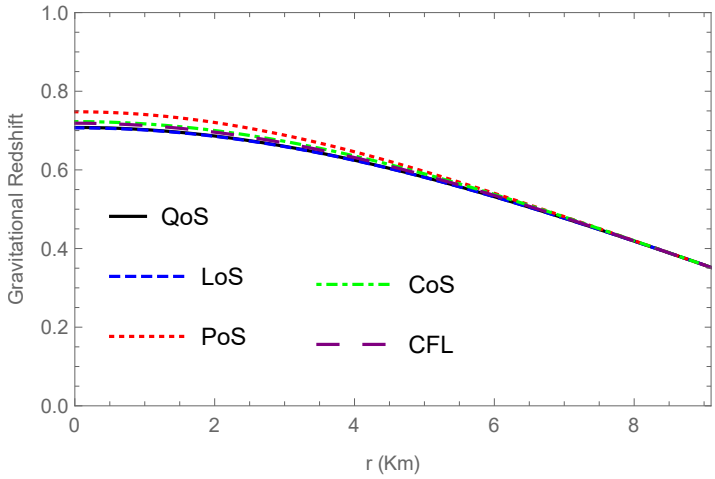

Figure 6.9: Variation of Gravitational redshift against radial variable r.

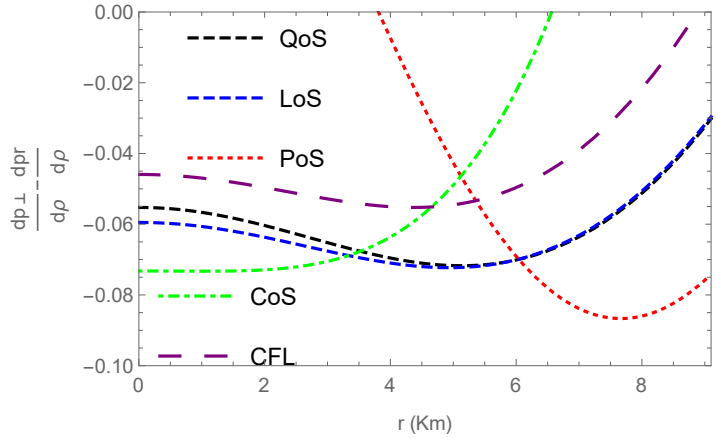

Figure 6.10: The causality condition with respect to the radial coordinate r.

Fig.(6.7) indicates that the strong energy condition $\rho - p_r - 2p_\perp > 0$ is satisfied througout the distribution. For a relativistic equilibrium model of a compact star is stable model, the adiabatic index $\Gamma = \frac{\rho+p_r}{p_r}\frac{dp_r}{d\rho} > \frac{4}{3}$ throughout the distribution. Fig.(6.8) indicates that the condition $\Gamma > \frac{4}{3}$ is satisfied for the star 4U 1820-30. For a relativistic star, it is expected that the redshift must be decreasing towards the boundary and finite throughout the distribution. Fig.(6.9) shows that gravitational redshift is decreasing throughout the star under consideration . Fig.(6.10) shows that $\frac{dp_\perp}{d\rho} - \frac{dp_r}{d\rho}$ is negative throughout the star for Quadratic, Linear and CFL equation of state. Fig.(6.11), Fig.(6.12), Fig.(6.13), Fig.(6.14), Fig.(6.15) shows the graphical

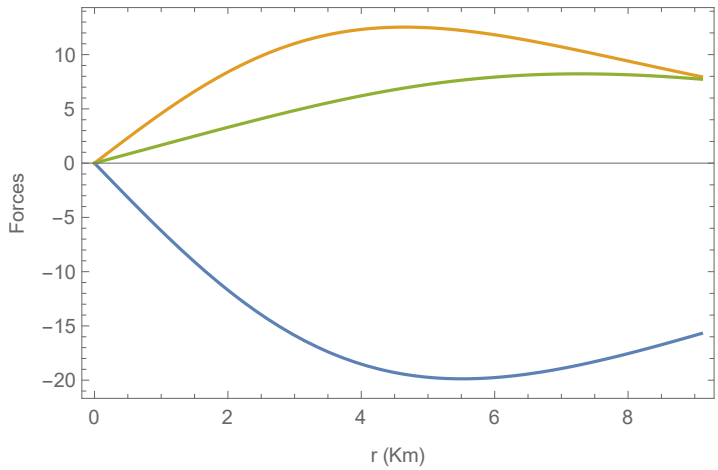

Figure 6.11: Variation of three forces (QoS) like Gravitational Force(Blue),Hydrostatic Force(Orange) and Anisotropic Force(Green) with respect to the radial coordinate r.

representation of three distinct forces for all equation of state linear, quadratic, polytrope, Chaplygin, and color-flavor-locked for the compact star 4U1820-30. The developed model can be used to study and compare the effect of the equation of states with different metric potentials.

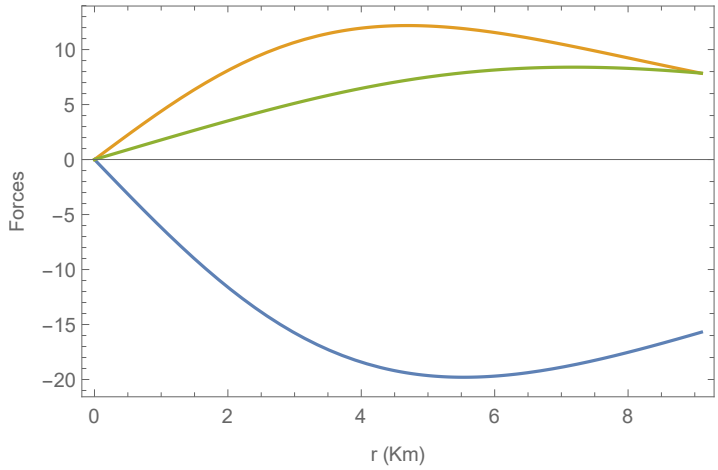

Figure 6.12: Variation of three forces (LoS) like Gravitational Force(Blue),Hydrostatic Force(Orange) and Anisotropic Force(Green) with respect to the radial coordinate r.

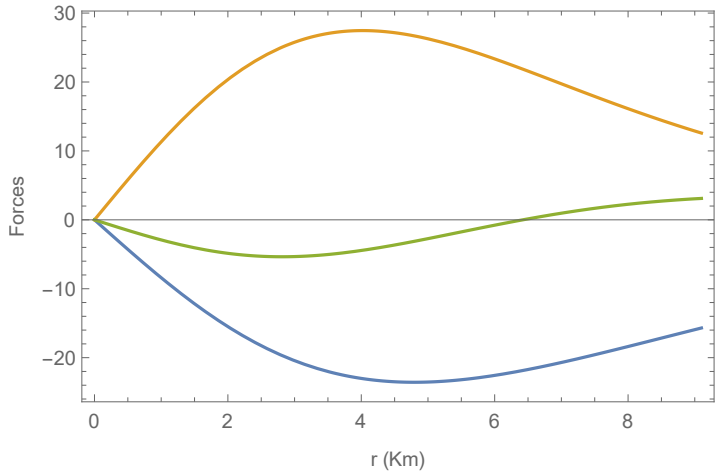

Figure 6.13: Variation of three forces (PoS) like Gravitational Force(Blue),Hydrostatic Force(Orange) and Anisotropic Force(Green) with respect to the radial coordinate r.

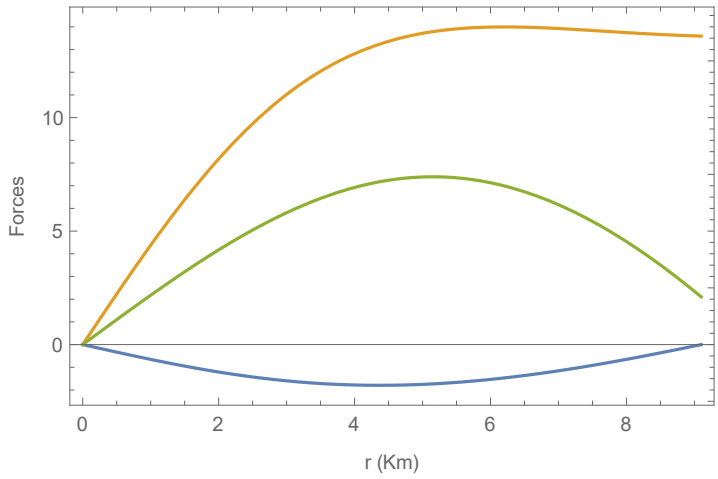

Figure 6.14: Variation of three forces (CoS) like Gravitational Force(Blue),Hydrostatic Force(Orange) and Anisotropic Force(Green) with respect to the radial coordinate r.

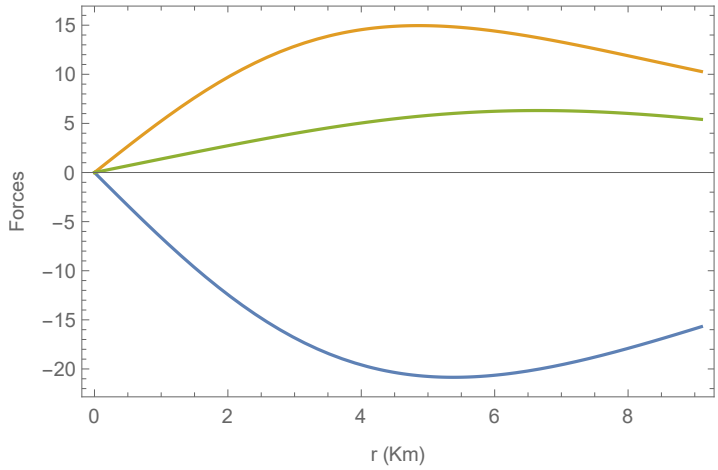

Figure 6.15: Variation of three forces (CFL) like Gravitational Force(Blue),Hydrostatic Force(Orange) and Anisotropic Force(Green) with respect to the radial coordinate r.